Theory of transformation thermal convection for creeping flow in porous media: Cloaking, concentrating, and camouflage

Gaole Dai, Jin Shang, and Jiping Huang*

Department of Physics, State Key Laboratory of Surface Physics, and Key Laboratory of Micro and Nano Photonic Structures (MOE), Fudan University, Shanghai 200433, China and Collaborative Innovation Center of Advanced Microstructures, Nanjing 210093, China

(Received 31 May 2017; revised manuscript received 8 November 2017; published 20 February 2018)

Heat can transfer via thermal conduction, thermal radiation, and thermal convection. All the existing theories of transformation thermotics and optics can treat thermal conduction and thermal radiation, respectively. Unfortunately, thermal convection has seldom been touched in transformation theories due to the lack of a suitable theory, thus limiting applications associated with heat transfer through fluids (liquid or gas). Here, we develop a theory of transformation thermal convection by considering the convection-diffusion equation, the equation of continuity, and the Darcy law. By introducing porous media, we get a set of equations keeping their forms under coordinate transformation. As model applications, the theory helps to show the effects of cloaking, concentrating, and camouflage. Our finite-element simulations confirm the theoretical findings. This work offers a transformation theory for thermal convection, thus revealing novel behaviors associated with potential applications; it not only provides different hints on how to control heat transfer by combining thermal conduction, thermal convection, and thermal radiation, but also benefits mass diffusion and other related fields that contain a set of equations and need to transform velocities at the same time.

DOI: 10.1103/PhysRevE.97.022129

I. INTRODUCTION

With the advent of the energy crisis, nonrenewable energy resources are decreasing, and they are producing more and more waste heat. Thus, an efficient control of heat transfer becomes particularly crucial. It is well known that the heat can generally transfer via three mechanisms, namely, thermal conduction, radiation, and convection.

Thermal conduction has been extensively studied by developing the theories of transformation thermotics [1–12]. As a result, some novel thermal metamaterials such as thermal cloaks and thermal camouflage [1–11], thermal concentrators [3], thermal rotators [3], macroscopic thermal diodes [10], and thermal transparency [12] have been theoretically designed and/or experimentally realized [3–11], which pave a new way to efficiently control heat conduction. With the help of optimization techniques, the concepts of cloaking, concentrating, and rotating have been successfully realized in electronics such as guiding heat flow in multilayer printed circuit boards and improving the efficiency of thermoelectric generators [13,14]. Existing theories of transformation optics [15,16] can be adopted to describe thermal radiation, which is essentially associated with electromagnetic waves. However, the thermal convection has seldom been touched in transformation theories [17], even though transformation theories (say, transformation thermotics and transformation optics as mentioned above) have been shown to be powerful for revealing novel behaviors like cloaking, concentrating, or camouflage. This is because of the lack of a suitable theory for transforming thermal convection. The difficulty might be that one should consider a set of complex equations at the same time since the flow of fluid can influence heat transfer. In contrast, in the case of thermal conduction, one only needs to transform the Fourier law. This fact largely limits applications associated with heat transfer through fluids (liquid or gas), which includes the process of thermal convection.

Actually, the theory of transformation thermotics [1] is a thermal-conduction analogy of transformation optics [15]; the latter is based on the fact that the Maxwell equations can keep their forms under coordinate transformation. In principle, if we have a set of equations with form invariance in different coordinate systems, we can also get a self-consistent theoretical framework to control thermal convection (corresponding to heat transfer with flow movement). However, the challenge is that the equations for electric fields and magnetic fields have the same form while the equations considered in this work do not. To this end, we overcome this challenge, and establish a theory of transformation convection (which is particularly for a forced thermal convection in porous media as an initial work in thermal convection) by considering the convection-diffusion equation, the Navier-Stokes equation, or the Darcy law.

II. THEORY

For treating heat transfer in fluids, we start by modifying the equation of heat conduction for incompressible flow without heat sources (neglecting the viscous dissipation term) [18,19] as

$$\rho C_p \nabla \cdot (\vec{v} T) = \nabla \cdot (\eta \nabla T), \tag{1}$$

where ρ, C_p, η, and $\vec{v}$ are, respectively, the density, specific heat at constant pressure, thermal conductivity of fluid materials, and the velocity of fluids. As is known, $\rho C_p \nabla \cdot (\vec{v} T)$ is the term

*jphuang@fudan.edu.cn

due to advection. Equation (1) is just the convection-diffusion equation. For simplicity, here we make some assumptions that the flow is laminar and Newtonian and that the density will not change with temperature.

For the coordinate transformation $\{x_i\} \to \{y_j\}$ and the associated Jacobian matrix $\mathbf{J} = \frac{\partial(y_1,y_2,y_3)}{\partial(x_1,x_2,x_3)}$, we can write [18]

$$\rho C_p \sum_j \frac{\partial}{\partial y_j}\left(\frac{1}{\det \mathbf{J}} \sum_i J_{ij}^{\intercal} v_i T\right) = \sum_{ijkl} \frac{\partial}{\partial y_k}\left(\frac{1}{\det \mathbf{J}} J_{ki}\eta_{ij} J_{jl}^{\intercal} \frac{\partial T}{\partial y_l}\right). \tag{2}$$

Let $\vec{v}' = \frac{\mathbf{J}^{\intercal}\vec{v}}{\det \mathbf{J}}$ and $\eta' = \frac{\mathbf{J}\eta\mathbf{J}^{\intercal}}{\det \mathbf{J}}$, and we can achieve

$$\rho C_p[\nabla' \cdot (\vec{v}'T)] = \nabla' \cdot (\eta' \nabla' T). \tag{3}$$

Equations (1) and (3) have the same form, so we can develop transformation thermotics by including heat convection.

Now, the key problem is how to realize both velocity distribution $\vec{v}'(\vec{r},t)$ and anisotropic thermal conductivity η' of fluid materials. Generally, in order to describe the state of fluids completely, we need to know the velocity $\vec{v}$ and any two thermodynamic quantities such as ρ and pressure p, which are determined by Eq. (1) together with Navier-Stokes equations and the equation of continuity [19]

$$(\vec{v}\cdot\nabla)\vec{v} = -\frac{1}{\rho}\nabla p + \frac{\beta}{\rho}\nabla\cdot\nabla\vec{v}, \tag{4}$$

$$\nabla\cdot\vec{v} = 0. \tag{5}$$

Here β is the dynamic viscosity. For simplicity, we have assumed $\vec{v}(\vec{r},t) = \vec{v}(\vec{r})$ and $\rho(\vec{r},t) \equiv \rho$. However, Eq. (5) can keep its form under coordinate transformation while Eq. (4) does not in most cases, even though we can neglect nonlinear term $(\vec{v}\cdot\nabla)\vec{v}$ when Reynolds number Re is small (a similar case as the elastic equation in [20]). It also remains a difficulty in experiments to make η' anisotropic in fluids, while this has been done successfully in heat conduction of solid materials. Fortunately, recent advances on velocity control [21] inspire us to consider heat transfer and velocity control in porous media at the same time.

In saturated porous media, we have a set of equations for steady flow as [22,23]

$$\rho_f C_{p,f}(\vec{v}\cdot\nabla T) = \nabla\cdot(\eta_m \nabla T), \tag{6}$$

$$\nabla p + \frac{\beta}{k}\vec{v} = 0, \tag{7}$$

$$\nabla\cdot\vec{v} = 0, \tag{8}$$

where k is the permeability and η_m is the effective thermal conductivity of porous media. In addition, ρ_f and $C_{p,f}$ denote, respectively, the density and specific heat at constant pressure of fluid material. By taking the volume-averaging method [23], the effective conductivity η_m is

$$\eta_m = (1-\phi)\eta_s + \phi\eta_f, \tag{9}$$

where ϕ is the porosity and η_f and η_s are, respectively, the thermal conductivity of fluid and solid material of porous media. In Eq. (6), we have assumed the local thermal equilibrium of fluids and solid materials, which means they have the same temperature at the contact point. Also, we take $\nabla\cdot(\vec{v}T) = \vec{v}\cdot\nabla T$ according to Eq. (8). Equation (7) is the Darcy law, which is valid when both Re and k are low enough. Owing to $\lambda = -\frac{k}{\beta}$ and $\vec{v}' = \mathbf{J}^{\intercal}\vec{v}/(\det\mathbf{J})$, it is easy to get under transformation $\{x_i\} \to \{y_j\}$,

$$v'_j = \sum_i J_{ji}v_i/(\det\mathbf{J}) = \sum_{ik} J_{ji}\lambda_{ki}\frac{\partial p}{\partial x_k}/(\det\mathbf{J}) = \sum_{ikl} J_{lk}\lambda_{ki}J_{ij}^{\intercal}\frac{\partial p}{\partial y_l}/(\det\mathbf{J}), \tag{10}$$

which means $\vec{v}' = \lambda'\nabla' p$ and $\lambda' = \frac{\mathbf{J}\lambda\mathbf{J}^{\intercal}}{\det\mathbf{J}}$.

Equations (6)–(8) can keep their form under general coordinate transformation, so we can get the wanted temperature and velocity distribution without changing any property of fluid

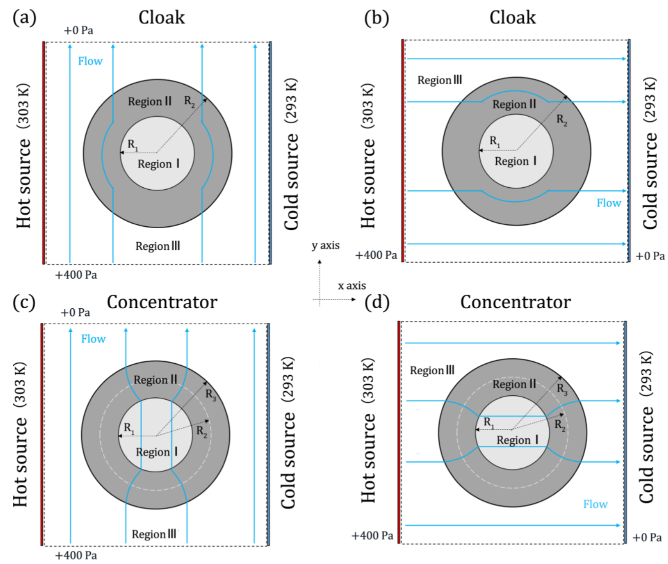

FIG. 1. Scheme of thermal cloak and concentrator. (a) Cloak with a background velocity in the y direction, as indicated by blue lines; (b) cloak with a background velocity in the x direction. (c) Concentrator with a background velocity in the y direction; (b) concentrator with a background velocity in the x direction. For cloaks, region I ($r' < R_1$) is a circular object to be cloaked while for concentrators, region I is the area where heat flux is concentrated. Region II is the transformation area for cloaks ($R_1 < r' < R_2$) or concentrators ($R_1 < r' < R_3$). For concentrators, the white broken-line circle with a radius of R_2 is a guideline for the transformation. In (a) and (b), the blue lines, representing streamlines of flow, would round the object. In (c) and (d), the blue lines would be concentrated in region I. Region III is the background area and we restrict it within a broken-line square with a side length of 8×10^{-5} m. We take $R_2 = 2R_1 = 2\times10^{-5}$ m for cloaks while $R_3 = 2R_1 = 2\times10^{-5}$ m for concentrators. For the cloak and concentrator, we put a hot heat source of 303 K on the left side of the square and a cold heat source of 293 K on the right. Background material parameters: $\rho_f = 10^3$ kg/m^3, $C_{p,f} = 5\times10^3$ J/(kg K), $\eta_f = 1$ W/(m K), $\rho_s =$ 500 kg/m^3, $C_{p,s} = 500$ J/(kg K), $\eta_s = 5$ W/(m K), and $\phi = 0.9$. Object to be cloaked in region I: $\rho = 10^4$ kg/m^3, $C_p = 5\times10^3$ J/(kg K), and $\eta = 200$ W/(m K).

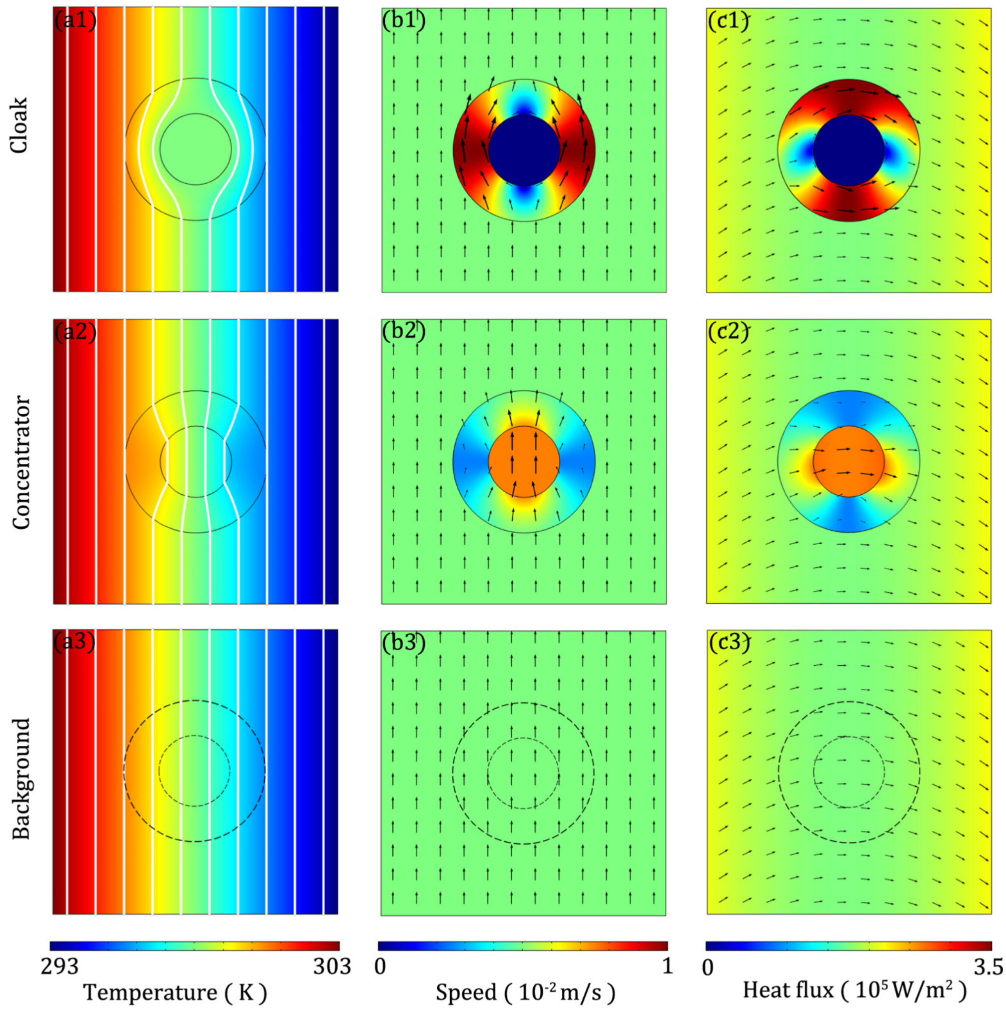

FIG. 2. Simulation results when the background velocity is along the y direction. The first row is for the cloak. (a1) describes the temperature distribution with white lines representing isotherms. (b1) shows the speed distribution and the arrows point in the direction of velocity, whose lengths are proportional to the speed. Similarly, (c1) shows the distribution of heat flux and the arrows point in the direction of heat flow, whose lengths are proportional to the amount of heat flux. The second and third rows represent the cases of concentrator and pure background, respectively. In (a3)–(c3), the two concentric circles only denote the position for the comparison with (a1)–(c1) and (a2)–(c2).

materials by transforming permeability

$$k' = \frac{\mathbf{J}k\mathbf{J}^{\intercal}}{\det \mathbf{J}}, \quad (11)$$

and the thermal conductivity

$$\begin{aligned} \eta'_m &= \frac{\mathbf{J}\eta_m\mathbf{J}^{\intercal}}{\det \mathbf{J}}, \\ \eta'_f &= \eta_f, \\ \eta'_s &= \frac{\eta'_m - \phi\eta_f}{1-\phi}. \end{aligned} \quad (12)$$

III. CLOAK AND CAMOUFLAGE

As a model application of the above theory, we first attempt to design a thermal cloak in two dimensions for simplicity. A cloak means it can shield the thermal scattering signals of an object in it [1–11]. For this purpose, we adopt the geometrical mapping [15] from the original region with radius r satisfying $0 < r < R_2$ to region II with radius r' satisfying $R_1 < r' < R_2$,

$$\begin{aligned} r' &= R_1 + \frac{R_2 - R_1}{R_2} r, \\ \theta' &= \theta, \end{aligned} \quad (13)$$

which is used to cloak an object located in region I ($0 < r < R_1$).

Writing all the parameters in Cartesian coordinates, we obtain the Jacobian matrix in region II as

$$\mathbf{J} = \begin{pmatrix} \cos\theta & -r'\sin\theta \\ \sin\theta & r'\cos\theta \end{pmatrix} \begin{pmatrix} \frac{R_2-R_1}{R_2} & 0 \\ 0 & 1 \end{pmatrix} \begin{pmatrix} \cos\theta & \sin\theta \\ -\frac{\sin\theta}{r} & \frac{\cos\theta}{r} \end{pmatrix}, \quad (14)$$

and it is not difficult to get $\det \mathbf{J} = \frac{R_2-R_1}{R_2}\frac{r'}{r}$. So the thermal conductivity in region II is $\eta'_m = \eta_m \frac{\mathbf{J}\mathbf{J}^{\intercal}}{\det \mathbf{J}}$ and similarly $k' = k\frac{\mathbf{J}\mathbf{J}^{\intercal}}{\det \mathbf{J}}$.

Then we perform finite-element simulations, which combine heat transfer and the Darcy law, by using the commercial software COMSOL MULTIPHYSICS [24]. In COMSOL, we use two

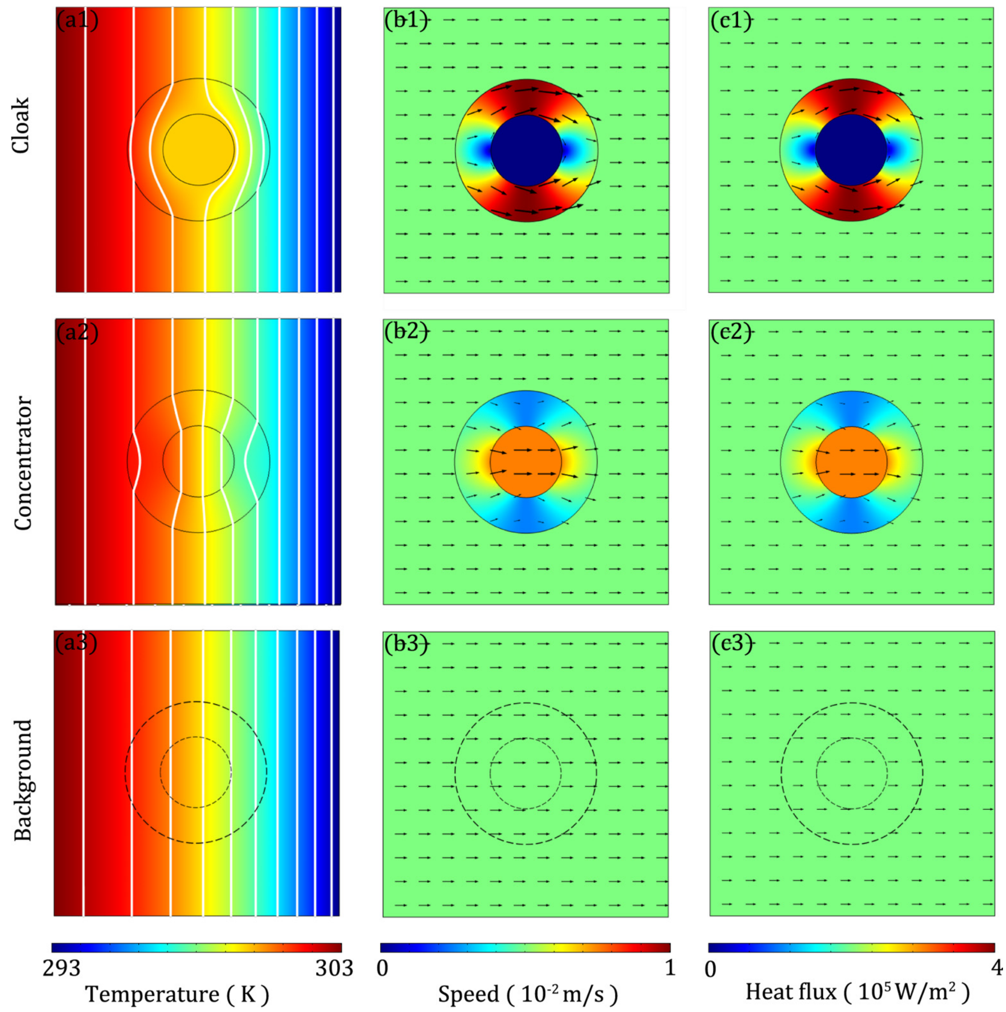

FIG. 3. Same as Fig. 2, but for the background velocity directed in the x direction.

templates: heat transfer in porous media and Darcy's law. The velocity field in heat transfer in porous media is generated by Darcy's law, meaning the equations are coupled with each other. Figure 1 shows the basic design for simulations. Since we study the models in two dimensions, all actual velocities can be decomposed into two eigenvectors along the x direction and the y direction. To compare the temperature distribution more straightforwardly and conveniently, we take a uniform horizontal or vertical velocity distribution as basic solutions.

According to Eq. (7), a pressure difference Δp added on the boundary of region III will generate a uniform velocity distribution in homogeneous medium. The parameters of fluid material are set with a reference of water, shown in the caption of Fig. 1 and we can also set the dynamic viscosity as $\beta = 10^{-3}$ Pa s. Besides, we take $k = 10^{-12}$ m^2 (this value is equal to 1 Darcy and is common in nature) and $\Delta p = 400$ Pa for modeling Darcy's law in COMSOL. It is easy to find that the background speed is $v = 5 \times 10^{-3}$ m/s with directions along the x axis and the y axis, respectively, if Δp is put horizontally and vertically (see Fig. 1). In all these cases, Reynolds numbers take $\mathrm{Re} = \frac{\rho R_2}{\beta} v = 0.1 \ll 1$ and $k \ll (R_2)^2$ so Darcy's law is solid here.

The simulation results are shown in Figs. 2 and 3. Firstly we consider the condition that background velocity $\vec{v}$ is in the y direction (see Fig. 2). Comparing the first row (cloak) and third row (pure background), we find that the distribution of temperature is the same in region III, and so are the distributions of velocity and heat flux. Also, the cloak has a zero-temperature gradient in region I, so in Fig. 2(c1) the heat flux is zero in region I. Actually, we have realized the cloaking of an object in both velocity and temperature fields simultaneously. The conclusion holds the same for the case with a background velocity $\vec{v}$ in the x direction, which can be seen in Fig. 3. What is more, we can see that the difference between the results of horizontal and vertical basic solutions lies in the horizontal shift of the pattern of temperature distribution. Moreover, the directions of heat flux caused by convection and conduction are parallel for horizontal basic solutions, while perpendicular to each other for vertical basic solutions.

Based on the same principle, thermal camouflage, which has been realized in heat conduction [8,9], can also be designed for thermal convection. Different from thermal cloak, the background for camouflage can be inhomogeneous and consisted of arbitrary compositions and geometries. Now we add four isolated solid objects in region III in the previous model of thermal cloak and observe the thermal signals scattered by the four objects. In Figs. 4 and 5, we show the simulation results for a given pressure difference in different directions. It can be

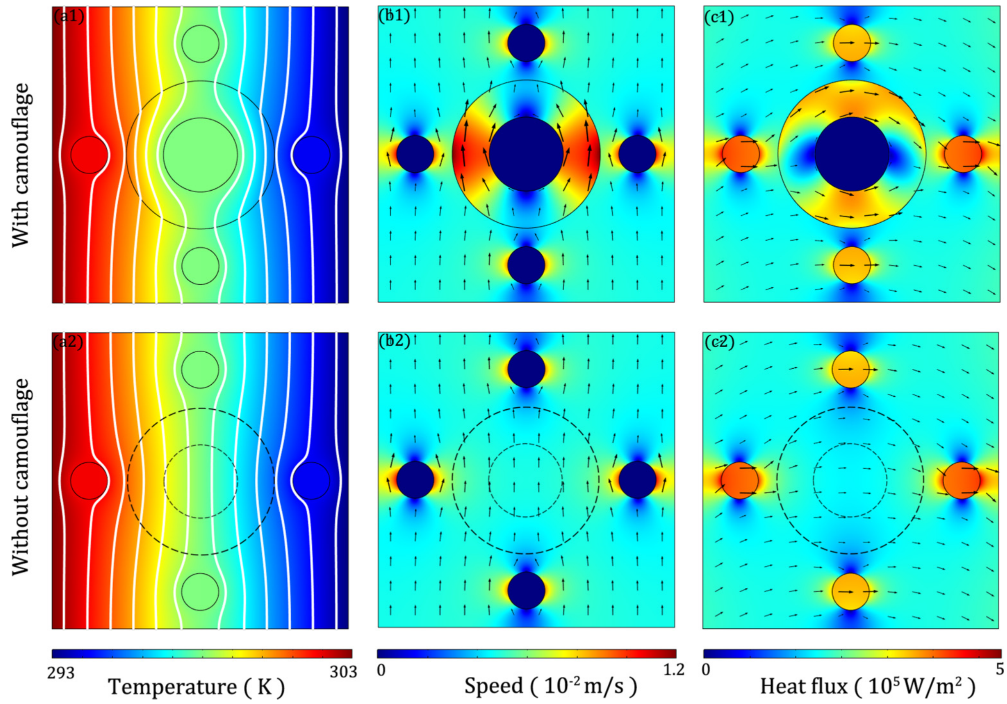

FIG. 4. Simulation results of thermal camouflage for the y-directed background velocity. (a1)–(c1) [or (a2)–(c2)] respectively describe the distributions of temperature, velocity, and heat flux in the existence (or absence) of a camouflage device. The four objects added in region III: $\rho = 10^4$ kg/m^3, $C_p = 5 \times 10^3$ J/(kg K), and $\eta = 200$ W/(m K).

found that the temperature signals (together with the velocity and heat flux signals) in region III are the same for the cases with and without camouflage devices, which means we can use this method to make the cloaked object behave as the four isolated solid objects in the background in the perspectives of heat and mass transfer.

IV. CONCENTRATOR

A thermal concentrator for heat conduction [3] can be used to enhance the temperature gradient (which means an enlarged heat flux) in a given area. When taking convection into account, we may realize the same effect. To proceed, we consider

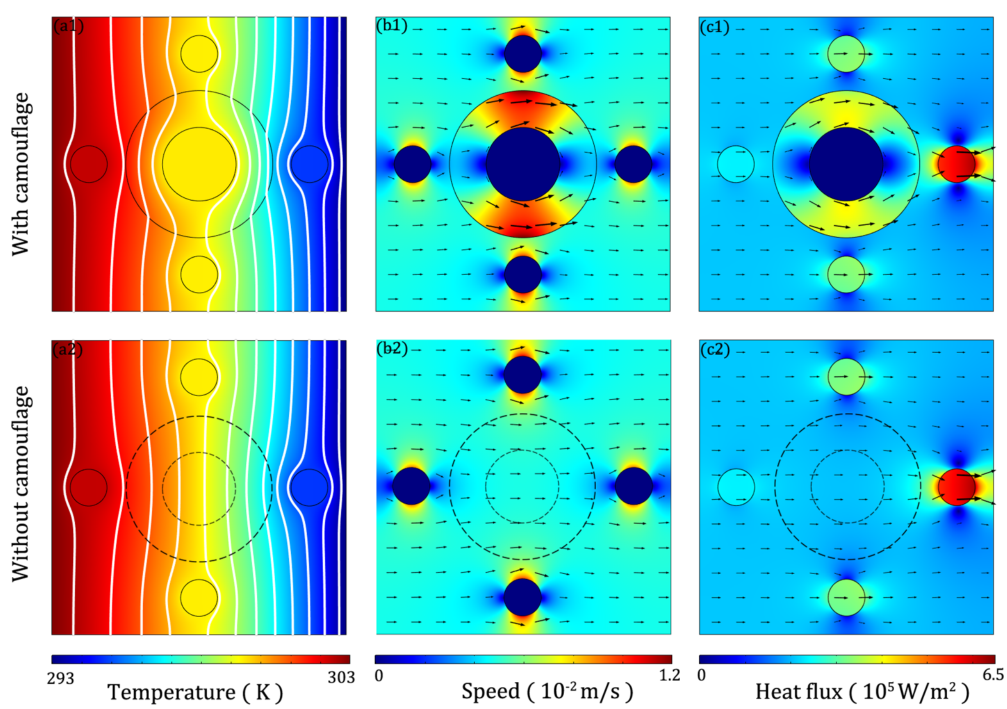

FIG. 5. Same as Fig. 4, but for the x-directed background velocity.

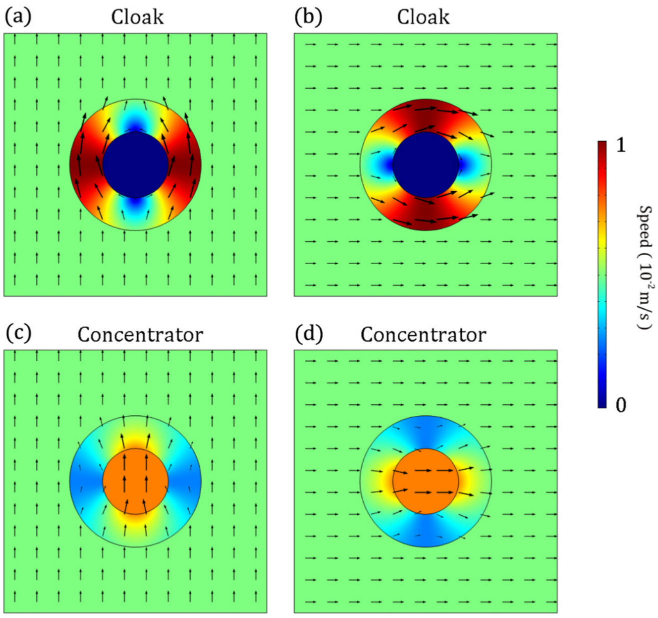

FIG. 6. Theoretical result of velocity distribution for cloak with background velocity in the (a) y or (b) x direction, and for a concentrator with background velocity in the (c) y or (d) x direction. The simulation results shown in Figs. 2(b1) and 2(b2) [or Figs. 3(b1) and 3(b2)] agree well with (a),(c) [or (b),(d)].

another geometrical transformation [25]

$$r' = \frac{R_1}{R_2} r \quad \text{as} \quad r < R_2,$$
$$r' = \frac{R_1 - R_2}{R_3 - R_2} R_3 + \frac{R_3 - R_1}{R_3 - R_2} r \quad \text{as} \quad R_2 < r < R_3, \tag{15}$$

which squeezes the region $0 < r < R_2$ to region I ($r' < R_1$) and then stretches the region $R_2 < r < R_3$ to region II ($R_1 < r' < R_3$).

The Jacobian matrices are

$$\mathbf{J}_1 = \begin{pmatrix} \frac{R_1}{R_2} & 0 \\ 0 & \frac{R_1}{R_2} \end{pmatrix} \tag{16}$$

for region I and

$$\mathbf{J}_2 = \begin{pmatrix} \cos\theta & -r'\sin\theta \\ \sin\theta & r'\cos\theta \end{pmatrix} \begin{pmatrix} \frac{R_3-R_1}{R_3-R_2} & 0 \\ 0 & 1 \end{pmatrix} \begin{pmatrix} \cos\theta & \sin\theta \\ -\frac{\sin\theta}{r} & \frac{\cos\theta}{r} \end{pmatrix} \tag{17}$$

for region II. It is easy to obtain

$$\frac{\mathbf{J}_1\mathbf{J}_1^\mathsf{T}}{\det \mathbf{J}_1} = \begin{pmatrix} 1 & 0 \\ 0 & 1 \end{pmatrix}. \tag{18}$$

So in region I ($r' < R_1$), we do not need to change k or η.

Again we set $R_3 = 2R_1 = 2 \times 10^{-5}$ m and $R_2 = 1.5 \times 10^{-5}$ m. All the other parameters are the same as for the case of thermal cloak. We simulate two cases with different velocity directions. The simulation results based on the COMSOL MULTIPHYSICS are shown in Figs. 2 and 3. We can see that the heat flux in region I gathers because of the increased temperature gradient and the amplified velocity in the same region. Meanwhile, in region III of Figs. 2(a2)–2(c2) and Figs. 3(a2)–3(c2), the temperature, velocity, and heat flux are also same as those for the cases of pure background shown in Figs. 2(a3)–2(c3) and Figs. 3(a3)–3(c3).

V. DISCUSSION AND CONCLUSION

According to our transformation theory, we can directly write velocity in region II as

$$\vec{v}\,' = \frac{R_2}{R_2 - R_1} \begin{pmatrix} \frac{r'-R_1}{r'}(v_x \cos^2\theta + v_y \sin\theta\cos\theta) + (v_x \sin^2\theta - v_y \sin\theta\cos\theta) \\ \frac{r'-R_1}{r'}(v_x \sin\theta\cos\theta + v_y \sin^2\theta) + (-v_x \sin\theta\cos\theta + v_y\cos^2\theta) \end{pmatrix}. \tag{19}$$

Here we use $\vec{v}\,' = \mathbf{J}^\mathsf{T}\vec{v}/\det\mathbf{J}$.

For concentrator, the theoretical velocity in region II is

$$\vec{v}\,'_2 = \frac{R_3 - R_2}{R_3 - R_1} \begin{pmatrix} \frac{r'+R_3}{r'}(v_x \cos^2\theta + v_y \sin\theta\cos\theta) + (v_x \sin^2\theta - v_y \sin\theta\cos\theta) \\ \frac{r'+R_3}{r'}(v_x \sin\theta\cos\theta + v_y \sin^2\theta) + (-v_x \sin\theta\cos\theta + v_y\cos^2\theta) \end{pmatrix} \tag{20}$$

and in region III

$$\vec{v}\,'_1 = \frac{R_2}{R_1}\vec{v}. \tag{21}$$

Since $R_1 < R_2$, the velocity in region I ($r' < R_1$) is amplified indeed. We plot the velocity distributions in Fig. 6. Clearly, the velocities generated by the Darcy law, as shown in Figs. 2(b1) and 2(b2) and Figs. 3(b1) and 3(b2), agree perfectly with Fig. 6. Namely, controlling velocity distribution by using the porous media can meet the theoretical requirements of velocity distribution.

We have set the background speed as $v = 5 \times 10^{-3}$ m/s and thus the Reynolds number is 0.1. Actually, when considering the thermal cloak or concentrator, the biggest speed is $v = 1 \times 10^{-2}$ m/s or $v = 0.75 \times 10^{-3}$ m/s, meaning that the corresponding Reynolds number is 0.2 or 0.15, where Darcy's law does not break down. Also, the low Reynolds number means that the friction-inertia term in Eq. (1) can be neglected, which holds for the parameters adopted in this work. Some recent works [21,26–28] discuss how to manipulate flows of higher Reynolds numbers in the presence or absence of porous media, such as Brinkman-Stokes flow and small Reynolds number turbulent flow (Re ≈ 100–10 000), whose methods both theoretically and experimentally might be helpful to promote further studies of controlling heat flow in more universal cases such as atmospheric circulation, oceanic circulation, mantle convection, and hydrologic cycle.

In our simulation, the velocity is generated by a pressure difference on the boundary, which actually means forced convection. In general, convection mainly consists of natural convection, forced convection, and mixed convection. As an initial attempt, our focus of this work is on the forced convection and for simplicity, we take density as a constant everywhere. The present consideration can be extended to treat natural convection and mixed convection, which is subjected to further research. Also, applying Darcy's law means we now consider small Reynolds numbers. Also we have to point out that by far the transformation theory has not been applied in the nanometer or molecular scale where Fourier's law breaks down. This is a topic of intense interest now [29–33] and how to control heat transfer in such microcosmic level is not a completely solved problem, although some advances have been made using the theories of phononics [34–39].

In this work, the temperature distribution is smooth and its gradient (and the velocity) is also continuous except that on the boundary of region II (where the tangential component may be discontinuous but the normal component is still continuous). Thus we can resort to the effective medium theory. Also, it is worth mentioning that when ϕ takes extreme values like 0.9 as adopted in this work, the present effective medium theory agrees with two well-known forms of effective medium theories, namely, the Bruggeman formula and the Maxwell-Garnett formula.

To sum up, we have established a transformation theory for manipulating thermal convection (in particular, forced convection in porous media), and revealed some novel behaviors of thermal convection, namely, concentrating, cloaking, and camouflage. They have potential applications (which still require future research): for example, the concentrating might help to collect heat energy from the environment with the help of a thermoelectric generator. This work provides hints on how to control heat transfer by combining conduction, radiation, and convection, and it also benefits the research of mass diffusion and other related fields that contain a set of equations and require the transformation of velocities simultaneously.

ACKNOWLEDGMENTS

We acknowledge the financial support by the National Natural Science Foundation of China under Grant No. 11725521, and by the Science and Technology Commission of Shanghai Municipality under Grant No. 16ZR1445100.

[1] C. Z. Fan, Y. Gao, and J. P. Huang, Shaped graded materials with an apparent negative thermal conductivity, Appl. Phys. Lett. **92**, 251907 (2008).
[2] T. Chen, C. N. Weng, and J. S. Chen, Cloak for curvilinearly anisotropic media in conduction, Appl. Phys. Lett. **93**, 114103 (2008).
[3] S. Narayana and Y. Sato, Heat Flux Manipulation with Engineered Thermal Materials, Phys. Rev. Lett. **108**, 214303 (2012).
[4] R. Schittny, M. Kadic, S. Guenneau, and M. Wegener, Experiments on Transformation Thermodynamics: Molding the Flow of Heat, Phys. Rev. Lett. **110**, 195901 (2013).
[5] H. Y. Xu, X. H. Shi, F. Gao, H. D. Sun, and B. L. Zhang, Ultrathin Three-Dimensional Thermal Cloak, Phys. Rev. Lett. **112**, 054301 (2014).
[6] T. C. Han, X. Bai, D. L. Gao, J. T. L. Thong, B. W. Li, and C. W. Qiu, Experimental Demonstration of a Bilayer Thermal Cloak, Phys. Rev. Lett. **112**, 054302 (2014).
[7] Y. G. Ma, Y. C. Liu, M. Raza, Y. D. Wang, and S. L. He, Experimental Demonstration of a Multiphysics Cloak: Manipulating Heat Flux and Electric Current Simultaneously, Phys. Rev. Lett. **113**, 205501 (2014).
[8] T. Han, X. Bai, J. T. L. Thong, B. Li, and C. W. Qiu, Full control and manipulation of heat signatures: Cloaking, camouflage and thermal metamaterials, Adv. Mater. **26**, 1731 (2014).
[9] T. Yang, X. Bai, D. Gao, L. Wu, B. Li, J. T. L. Thong, and C. W. Qiu, Invisible sensors: Simultaneous sensing and camouflaging in multiphysical fields, Adv. Mater. **27**, 7752 (2015).
[10] Y. Li, X. Y. Shen, Z. H. Wu, J. Y. Huang, Y. X. Chen, Y. S. Ni, and J. P. Huang, Temperature-Dependent Transformation Thermotics: From Switchable Thermal Cloaks to Macroscopic Thermal Diodes, Phys. Rev. Lett. **115**, 195503 (2015).
[11] X. Y. Shen, Y. Li, C. R. Jiang, and J. P. Huang, Temperature Trapping: Energy-Free Maintenance of Constant Temperatures as Ambient Temperature Gradients Change, Phys. Rev. Lett. **117**, 055501 (2016).
[12] X. He and L. Z. Wu, Thermal transparency with the concept of neutral inclusion, Phys. Rev. E **88**, 033201 (2013).
[13] E. M. Dede, P. Schmalenberg, T. Nomura, and M. Ishigaki, Design of anisotropic thermal conductivity in multilayer printed circuit boards, IEEE Trans. Compon., Packag., Manuf. Technol. **5**, 1763 (2015).
[14] E. M. Dede, P. Schmalenberg, C.-M. Wang, F. Zhou, and T. Nomura, Collection of low-grade waste heat for enhanced energy harvesting, AIP Adv. **6**, 055113 (2016).
[15] J. B. Pendry, D. Schurig, and D. R. Smith, Controlling electromagnetic fields, Science **312**, 1780 (2006).
[16] U. Leonhardt, Optical conformal mapping, Science **312**, 1777 (2006).
[17] S. Guenneau, D. Petiteau, M. Zerrad, C. Amra, and T. Puvirajesinghe, Transformed Fourier and Fick equations for the control of heat and mass diffusion, AIP Adv. **5**, 053404 (2015).
[18] S. Guenneau and T. M. Puvirajesinghe, Fick's second law transformed: One path to cloaking in mass diffusion, J. R. Soc., Interface **10**, 20130106 (2013).
[19] L. D. Landau and E. M. Lifshitz, *Fluid Mechanics*, 2nd ed. (Pergamon, London, 1987).
[20] G. W. Milton, M. Briane, and J. R. Willis, On cloaking for elasticity and physical equations with a transformation invariant form, New J. Phys. **8**, 248 (2006).
[21] Y. A. Urzhumov and D. R. Smith, Fluid Flow Control with Transformation Media, Phys. Rev. Lett. **107**, 074501 (2011).
[22] J. Bear, *Dynamics of Fluids in Porous Media* (Elsevier, New York, 1972).
[23] J. Bear and M. Y. Corapcioglu, *Fundamentals of Transport Phenomena in Porous Media* (Springer, Netherlands, 1984).
[24] COMSOL Multiphysics, http://www.comsol.com/.

[25] M. Rahm, D. Schurig, D. A. Roberts, S. A. Cummer, D. R. Smith, and J. B. Pendry, Design of electromagnetic cloaks and concentrators using form-invariant coordinate transformations of Maxwell's equations, Photonics Nanostruct. Fundam. Appl. **6**, 87 (2008).

[26] Y. A. Urzhumov and D. R. Smith, Flow stabilization with active hydrodynamic cloaks, Phys. Rev. E **86**, 056313 (2012).

[27] P. T. Bowen, Y. A. Urzhumov, and D. R. Smith, Wake control with permeable multilayer structures: The spherical symmetry case, Phys. Rev. E **92**, 063030 (2015).

[28] D. R. Culver, E. Dowell, D. R. Smithh, Y. A. Urzhumov, and A. Varghese, A volumetric approach to wake reduction: Design, optimization, and experimental verification, J. Fluids **2016**, 1 (2016).

[29] A. Dhar, Heat transport in low-dimensional systems, Adv. Phys. **57**, 457 (2008).

[30] D. M. Leitner, Thermal boundary conductance and rectification in molecules, J. Phys. Chem. B **117**, 12820 (2013).

[31] T. Zhang and T. Luo, Giant thermal rectification from polyethylene nanofiber thermal diodes, Small **11**, 4657 (2015).

[32] D. Segal and B. K. Agarwalla, Vibrational heat transport in molecular junctions, Ann. Rev. Phys. Chem. **67**, 185 (2016).

[33] H. D. Pandey and D. M. Leitner, Thermalization and thermal transport in molecules, J. Phys. Chem. Lett. **7**, 5062 (2016).

[34] B. Li, L. Wang, and G. Casati, Thermal Diode: Rectification of Heat Flux, Phys. Rev. Lett. **93**, 184301 (2004).

[35] B. Li, L. Wang, and G. Casati, Negative differential thermal resistance and thermal transistor, Appl. Phys. Lett. **88**, 143501 (2006).

[36] L. Wang and B. Li, Thermal Logic Gates: Computation with Phonons, Phys. Rev. Lett. **99**, 177208 (2007).

[37] N. Li, J. Ren, L. Wang, G. Zhang, P. Hänggi, and B. Li, Phononics: Manipulating heat flow with electronic analogs and beyond, Rev. Mod. Phys. **84**, 1045 (2012).

[38] P. Ben-Abdallah and S. A. Biehs, Near-Field Thermal Transistor, Phys. Rev. Lett. **112**, 044301 (2014).

[39] V. Kubytskyi, S. A. Biehs, and P. Ben-Abdallah, Radiative Bistability and Thermal Memory, Phys. Rev. Lett. **113**, 074301 (2014).